

# NUMERICAL STUDIES OF A FLEXIBLE STRUCTURE SUBJECTED TO VORTEX-INDUCED VIBRATIONS

**Guilherme R. Franzini, guilherme.franzini@poli.usp.br**

**André L.C. Fujarra, afujarra@usp.br**

Department of Naval Architecture and Ocean Engineering, EP, University of São Paulo

**Celso P. Pesce, ceppesce@usp.br**

Department of Mechanical Engineering, EP, University of Sao Paulo

## Fluid-Structure Interaction and Offshore Mechanics Laboratory - LIFE & MO

**Abstract.** *This work presents a numerical method and results obtained from numerical simulations of Vortex-Induced Vibration phenomenon (VIV) acting on a horizontal and flexible structure. A cable is free to oscillate only in the cross-flow direction. As the first part of the studies, simulations in free condition were done in order to evaluate eigenvalues and eigenmodes of this system. The obtained results were in agreement with the analytical solution for the horizontal cable dynamics. Subsequently, using a lumped-mass method, each segment of the zero bending stiffness structure is coupled by the lift force to a wake oscillator, defined as a van der Pol equation. Increasing the value of the uniform free stream velocity  $U$ , VIV phenomenon was excited on the segments of the structure. Classical curves of nondimensional amplitude and frequency as function of the reduced velocity were plotted, showing a good adherence with theoretical results. In a final set of simulations, the free stream velocity was linearly varied by means of a decreasing after an increasing slope-function. Using this approach, the whole lock-in range was swept in one simulation and applying the Hilbert-Huang Technique both the amplitude and frequency were evaluated instantaneously. The analysis showed a hysteresis behavior in the transition of the initial to the upper branch, more evident when the slope in the velocity variation is increased.*

**Keywords:** *Vortex-Induced Vibrations, numerical study, lumped-mass model, wake oscillator.*

## 1. INTRODUCTION

Vortex-Induced Vibrations (VIV) is a highly non-linear, self-excited and self-regulated phenomenon. In the offshore engineering, VIV is particularly important on the dynamics of risers and others structures. Due its self-limited and self-excited characteristics, it can lead to fatigue failure of these structures. It occurs when one has a viscous flow around a bluff-body, creating two shear layers, which interacting each other, generating a periodic vortex-shedding wake.

If the vortex-shedding frequency  $f_s$  is equal or close to one of the natural frequencies of the structure, a condition called lock-in occurs, in which the higher values of amplitude are observed. Bearman (1984) and Williamson and Govardhan (2004) are excellent references about the vortex-shedding mechanism.

Due its complex characteristics, VIV study is carried out in different approaches. Numerical approaches consists in solving the Navier-Stokes equation in a discrete domain. Experimental approaches employs small-scale models under controlled flow conditions in order to acquire and process times series of displacements, accelerations, pressures and forces, allowing the researchers to obtain non-dimensional coefficients, such as lift, drag and added-mass coefficients, oscillation frequencies and amplitudes. The analytical approaches employs mathematical equations aiming to emulate some desired properties of a structure subjected to VIV.

This work focus on the analytical approach, using a van der Pol equation in order to emulate the wake behavior. There are others models that can represent the wake. Some of them can be found in the dissertation by Cunha (2005). The wake behavior so emulated is self-limited and self-excited, obtained through a non-linear velocity-dependent damping term. The coupling wake and elastic oscillators is done by the lift force, and consists in an analytical solution for the VIV problem of a structure immersed in a viscous flow. Facchinetti et al (2004) brings others ways to model this coupling.

The results for natural frequency and mode shapes obtained by employing the discrete model for the cable were compared with the analytical results for horizontal cable dynamics (see Blevins (1984)). An estimated value of maximum amplitude of oscillation can be found as a function of the Reynolds number, the damping coefficient  $\zeta$  and the mass ratio  $m^*$ , using the 'modified Griffin plot'. For more details, see Govardhan and Williamson (2006).

Franzini et al (2008) presents experimental results for a rigid cylinder, free to oscillate only in cross-flow direction and subjected to a time-varying reduced velocity, constant Reynolds number. Results for the time-series of displacement were evaluated using the Hilbert-Huang Technique (see Huang et al (1998)). The results for the continuum curves of amplitude and frequency shows an important hysteresis.

## 2. PHENOMENOLOGICAL MODEL

### 2.1 Structural Oscillator

A horizontal and zero bending stiffness flexible structure is treated in this work through a lumped-mass model, with  $N$  nodes, separated by a distance  $\Delta$ , subjected to axial tension  $T$ . It is considered vibrations only in cross-flow direction. Using Lagrange's equation and considering small amplitudes of oscillation, compared to the length of the cable, the following linearized equation is obtained for the structural oscillator:

$$m[\mathbf{I}]\{\ddot{y}\} + [\mathbf{C}]\{\dot{y}\} + [\mathbf{K}]\{y\} = \{Q\} \quad (1)$$

Where:

$$[\mathbf{M}] = m[\mathbf{I}],$$

$$[\mathbf{K}] = \frac{T}{\Delta} \begin{pmatrix} 1 & -1 & 0 & \dots & 0 \\ -1 & 2 & -1 & \dots & 0 \\ 0 & -1 & 2 & -1 & \dots \\ \vdots & \vdots & \vdots & \vdots & \vdots \\ 0 & 0 & \dots & -1 & 1 \end{pmatrix}$$

$$[\mathbf{C}] = c \begin{pmatrix} 1 & -1 & 0 & \dots & 0 \\ -1 & 2 & -1 & \dots & 0 \\ 0 & -1 & 2 & -1 & \dots \\ \vdots & \vdots & \vdots & \vdots & \vdots \\ 0 & 0 & \dots & -1 & 1 \end{pmatrix}$$

The variable  $m$  is the mass of each component of the discrete system, including the structural mass  $m_s$  and the effect of the potential added mass  $m_a^{pot} = C_a \rho \pi \frac{D^2}{4}$ , where  $C_a$  is the potential added mass coefficient. For cylinders  $C_a^{pot} = 1$ , see Blevins (2001).

### 2.2 Parra and Aranha's Wake Oscillator model

As mentioned in the introduction, a van der Pol equation was adopted in order to describe the wake oscillator. In this paper, the Iwan & Blevins model was applied according to modifications proposed by Parra and Aranha (1996) described in this section.

Parra and Aranha's model employs a fictitious variable  $w$  meant for representing the wake dynamics. The natural frequency of the non-linear oscillator is defined as the Strouhal frequency,  $\omega_s = 2\pi St \frac{U}{D}$ , where  $St$  is the Strouhal number. The damping is the non-linear term, dependent of the square of the velocity of the wake variable. The damping term is defined by Eq. 2

$$c_w = 2m_f \omega_s \alpha_1 \left( \frac{4\alpha_2}{3\gamma U^2} \dot{w}^2 - 1 \right) \quad (2)$$

Where  $m_f = \frac{\alpha_0 \rho \pi D^2}{4}$  is the "inertia" of the wake oscillator,  $U$  is the flow velocity,  $\gamma$  is the modal coefficient and  $\alpha_0$ ,  $\alpha_1$ ,  $\alpha_2$  are coefficients determined by experiments. Those coefficients are presented in Tab. 1.

Table 1. Wake oscillator coefficients

Coefficient	Value
$St$	0,2
$\alpha_0$	0,48
$\alpha_1$	0,05
$\alpha_2$	3,01
$\alpha_4$	0,75

Finally, the lift force, which is responsible for the coupling between the structural and wake oscillators, is dependent of the 'angle of attack' defined by the structural and wake displacements. If  $\dot{w} \ll \dot{y}$ , the angle of attack can be defined as  $\frac{\dot{w} - \dot{y}}{U}$ , and the lift force can be written as Eq. 3

$$f_l = \frac{1}{2} \rho U^2 D \alpha_4 \left( \frac{\dot{w} - \dot{y}}{U} \right) \quad (3)$$

Where  $\rho$  is the fluid density and  $\alpha_4$  is another coefficient determined by experiments. Then, the wake oscillator, as described in this section is defined by Eq. 4

$$m_f \ddot{w} + 2m_f \omega_s \alpha_1 \left( \frac{4\alpha_2}{3\gamma U^2} \dot{w}^2 - 1 \right) \dot{w} + (m_f \omega_s^2) w = \frac{1}{2} \rho U D \alpha_4 \dot{y} \quad (4)$$

### 2.3 Coupling between wake and structural oscillators

The coupling between the structural and wake oscillators done in this work consists in assembling, at each lumped-mass, a van der Pol oscillator as defined by Eq. 4. Three hypotheses were assumed:

- Lumped-mass point dynamics, such that  $\gamma = 1$  for all discrete masses.
- The coefficients defined by experiments  $\alpha_0, \alpha_1, \alpha_2, \alpha_4$  and  $St$  are the same for all lumped-mass nodes, given in Tab 1.
- The cable is not able to vibrate in two or more modes simultaneously.

The coupled system (Eq. 5), representing both wake and structural oscillator, was solved using a  $4^{th} - 5^{th}$  order Runge-Kutta method.

$$\begin{aligned} [\mathbf{M}] \{\ddot{y}\} + \left( [\mathbf{C}] + \frac{\rho U D \alpha_4}{2} [\mathbf{I}] \right) \{\dot{y}\} + [\mathbf{K}] \{y\} &= \frac{1}{2} \rho U D \alpha_4 \{\dot{w}\} \\ [\mathbf{Mf}] \{\ddot{w}\} + 2[\mathbf{Mf}] \omega_s \alpha_1 \left( \frac{4\alpha_2}{3U^2} \{\dot{w}\}^2 - 1 \right) \{\dot{w}\} + [\mathbf{Mf}] \omega_s^2 \{w\} &= \frac{1}{2} \rho U D \alpha_4 \{\dot{y}\} \end{aligned} \quad (5)$$

Where  $[\mathbf{Mf}] = m_f [I]$  can be interpreted as a inertia matrix of the fluid.

## 3. SIMULATIONS AND RESULTS

As mentioned in the abstract, three set of simulations were carried out with 50 lumped-masses. The parameters of the flexible structure were kept constant and are presented in Tab.2.

Table 2. Parameters for simulations.

Parameter	Value	Unit
$T$	63, 62	$N$
$D$	15	$mm$
$c$	0	$Ns/m$
$L$	800	$mm$
$m_s$	0, 163	$kg/m$
$\rho$	1000	$kg/m^3$
$m^* = \frac{4m_s}{\rho \pi D^2}$	0, 92	

The approximated values for the eigenmodes and eigenfrequencies are evaluated by solving the discrete eigenvalue problem  $[\mathbf{M}]^{-1}[\mathbf{K}]$ . Results can be found in Fig.1, for the first fours natural frequencies. One can note the good agreement between the eigenfrequencies obtained numerically and the ones obtained through analytical formulation given by Eq.6, where  $i$  represents the natural mode. The modal shape for the same structure is  $\psi_i(z) = \sin(\pi i \frac{z}{L})$  and also shows very good agreement with the eigenvectors numerically obtained.

$$f_n^i = \frac{i}{2\pi L} \sqrt{\frac{T}{m}} \quad (6)$$

### 3.1 Free-oscillating simulations

Free-oscillation simulations consisted in giving an initial condition for the lumped-mass system different from the equilibrium. Two simulations were done. The first simulation gives to the mass at the mid section of the structure an initial displacement equal to one diameter, keeping other masses at rest.

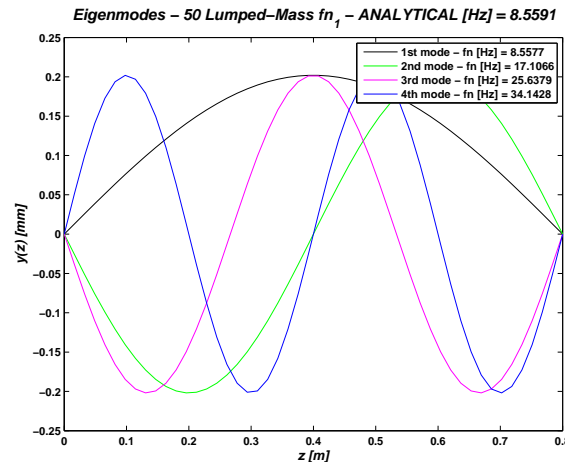


Figure 1. Eigenmodes and Eigenfrequencies

The results for free oscillation can be found in Fig. 2. Fig. 2(a) shows that, for the given initial condition, some natural frequencies appear in amplitude spectrum. These frequencies match the eigenfrequencies obtained through numerical analysis. If the initial condition of the structure matches with one of the natural mode shape, as can be observed in Fig. 2(b), just the corresponding natural frequency is observed in the amplitude spectrum. This fact is due to the orthogonality of the natural modes, as tension is constant along the cable length.

### 3.2 CLASSICAL VIV RESPONSE SIMULATIONS

The present section shows results obtained for the structure subjected to a uniform and constant-by-steps free stream velocity.

The structure is subjected to a free stream velocity in the range  $0.4 \leq U \leq 1.6 \text{ m/s}$ . This range is able to excite VIV in the structure at two first natural modes. The results for amplitude and frequency of oscillation are plotted as function of the reduced velocity  $V_r^1 = \frac{U}{f_n^1 D}$  in Fig. 3, where  $f_n^1$  represents the first eigenfrequency.

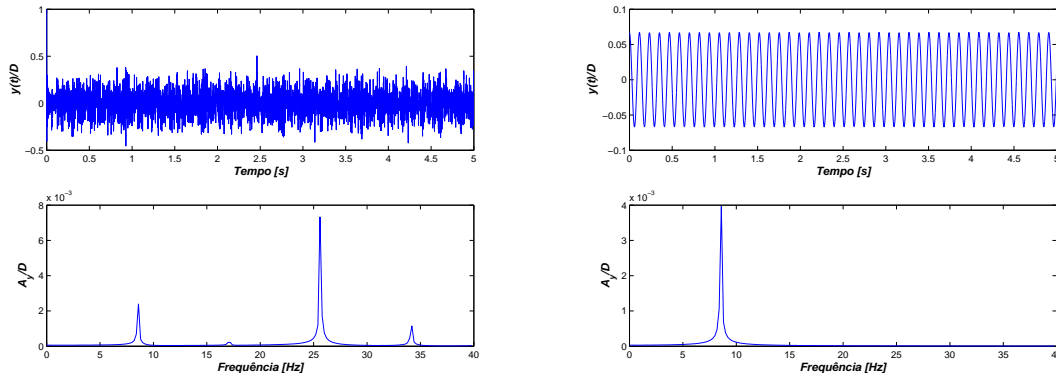
This figure shows a peak of amplitude  $\frac{A}{\gamma D}$  close to 1.7, for values of  $V_r^1 = 5.5$  and  $V_r^1 = 11$ , corresponding to the lock-in in the first and second modes respectively. As expected, no multi-modal vibration was observed in this simulation. The curve for  $f/f_n^1$  shows clearly the lock-in phenomenon, and the linear behavior outside the lock-in range.

At first amplitude peak, the corresponding Reynolds number approximately 10600. Using the 'modified Griffin plot', according Govardhan and Williamson (2006), the predicted amplitude response, for zero damping is 1.06. For the second peak of amplitude, we expected a maximum amplitude close to 1.17. The lower branch, see Khalak and Williamson (1999), in amplitude versus reduced velocity plot is not observed in the simulations. This is, actually, a draw back of the Iwan & Blevins model, which does not consider the variation of added mass with the reduced velocity. If included, this model variation enables the model to emulate the lower amplitude response branch, see Fujarra (2002).

### 3.3 SIMULATIONS WITH CONTINUOUS VARIATION OF FREE STREAM VELOCITY

The last set of simulations consisted in subjecting the structure to a uniform and time-dependent free stream velocity  $U(t)$ , which follows a slope function, increasing and then after decreasing the value of  $U(t)$ . Two conditions of  $U(t)$  were simulated, and the only difference between two conditions is the value of the slope (acceleration)  $\alpha$ . The Tab.3 shows the parameters for the simulations under variable  $U$ .

Accordingly, the reduced velocity also varies with time, so that both amplitude and frequency of oscillation are time-dependent. The time series of displacement can not be studied through Fourier Transform, because this technique gives no instantaneous information of amplitude and frequency. Instead this common technique provides information for the whole time interval under analysis, besides being strictly valid for stationary signals emerging from linear systems. In order to provide a time series of amplitude and frequency, the Hilbert-Huang Technique was chosen, see Huang et al (1998). The Hilbert-Huang Technique is a very powerful technique for nonlinear and non-stationeries signal analysis.



(a) Free oscillation simulation. Only the mass at mid section has initial displacement different from 0. (b) Free oscillation simulation. The initial displacement of the lumped-mass system follow equation  $y_0 = \sin\left(\pi \frac{z}{L}\right)$ .

Figure 2. Results for free-oscillations simulations.

Table 3. Definition of the simulations with variable free stream velocity.

Simulation	Range of U	$\alpha [m/s^2]$
Sim. 1	$0.4 \leq U \leq 1.6m/s$	0.08
Sim. 2	$0.4 \leq U \leq 1.6m/s$	0.16

Fig.5 shows the results for time series of displacement of the node positioned at  $L/4$ . There exist a clear hysteresis, despite the symmetric variation of  $U(t)$  with respect to time (increasing and decreasing with the same rate).

Figs.5(c) and 5(d) corresponding to the Intrinsic Mode Functions (IMFs), for each time series. The Intrinsic Mode Functions are the results obtained from the process called Empirical Mode Decomposition, in which the signal is decomposed in components based on time-scales, see Huang et al (1998). One can note that the whole energy of the signals is essentially contained in the first IMF. Considering only the first IMF of both signals, Figs.5(e) and 5(f) present the continuous curve of both amplitude and frequency VIV response as a function of the instantaneous reduced velocity  $V_r^1(t)$ .

Due the position of the chosen node, it is obvious that the second natural mode of vibration is more evident in Figs.5(e) and 5(f). Comparing Sim 1 and Sim 2 it is clear that the faster is the variation applied to the free stream velocity the more pronounced is the hysteresis. This is, therefore, inherent to the wake nonlinear oscillator model. The maximum value of  $A/\gamma D$  is close to 1.50 for both simulations, and occur at  $V_r^1(t) \approx 11$ , as expected for the second natural mode. This value is slightly smaller than the one obtained through classical simulations, which consists in increasing the free stream velocity by steps. Experiments in Franzini et al (2008) show the same behavior that is now emerging verified in the present simulation.

#### 4. CONCLUSIONS

This paper presented a mathematical model for the problem of a flexible cable subjected to Vortex-Induced Vibrations (VIV), free to oscillate only in cross-flow direction. The discrete structural oscillator was defined as a lumped-mass system, obtained using Lagrange's equation. The wake oscillator was defined as the one proposed by Parra and Aranha (1996). A van der Pol equation was employed for each lumped mass in order to describe the self-limited and self-excited character of the phenomenon. The coupling between structural and wake oscillators was modeled by the sectional lift force.

Two simulations of free and non-damped (structurally) oscillation were done. In the amplitude spectrum it has been observed the natural frequencies of the structure and the orthogonality of the natural modes, as expected by analytical results for this horizontal cable problem. The classical VIV simulation were carried out, in which the free-stream velocity is increased by steps. The peak of amplitude occurs at a value of reduced velocity which agrees with experimental results. The lower branch is not identified, and the peak of amplitude reaches a maximum value higher than the one predicted by

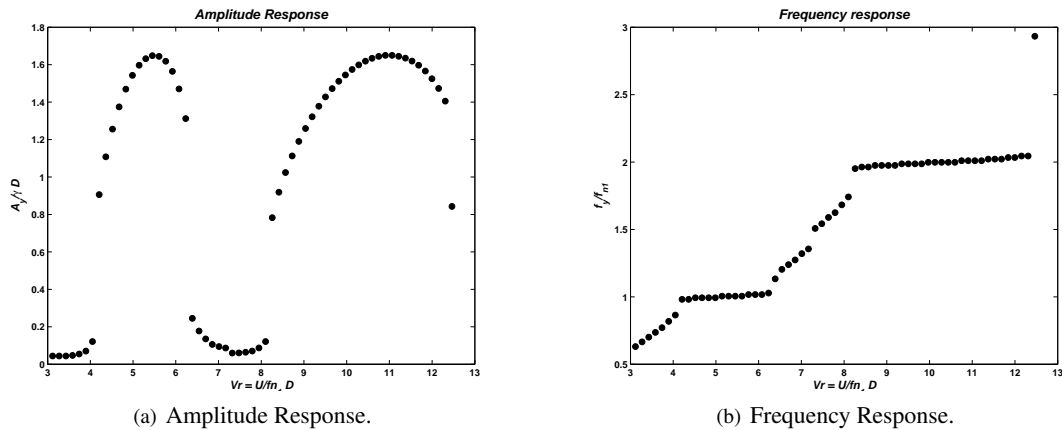


Figure 3. Results for free-oscillations simulations.

the "modified Griffin plot".

The simulations with time-dependent free stream velocity  $U(t)$  allow to obtain a time continuous curve of amplitude and frequency versus instantaneous reduced velocity. At this condition, the maximum value of amplitude occurs at the same reduced velocity observed in the step-by-step velocity increasing. Two values of slope for the velocity variation were simulated, and it was noted that the higher the value of the slope, the more pronounced is the hysteresis between small and high amplitude response regions. This fact was also noted in previously experiments. Another experimental fact observed in the simulations was the slightly small maximum amplitude for the continuous variation if compared with the classical condition of VIV simulation, what should be expected due to the inertia of the system to variations in  $U(t)$ .

Further works plan to include analytical studies of VIV of a flexible cylinder free to oscillate both in cross-flow direction and in-line direction. Simulations under parametric excitation, as in a Mathieu type oscillator, are also planned. Finally, improvements in the phenomenological model, aiming to identify the lower branch and to obtain multi-modal vibration are in course.

## 5. ACKNOWLEDGEMENTS

The first author would like to acknowledge FAPESP (São Paulo Research Foundation) for the PhD financial support, through process 2008/00688-4.

## 6. REFERENCES

- Bearman, P.W., 1984. "Vortex Shedding from Oscillating Bluff Bodies", Annual Review of Fluids Mechanics, Vol. 16, pp. 195-222.
- Blevins, R., 1984. "Formulas for Natural Frequency and Mode Shape".
- Blevins, R., 2001. "Flow induced vibration". Krieger Publishing, Malabar, FL.
- Cunha, L.D., 2005. "Vibração Induzida por Vórtices: Análise Crítica dos Modelos Fenomenológicos", MsC Dissertation, Escola Politécnica, University of São Paulo, São Paulo, Brazil.
- Facchinetti, E. L., de Langre, E. and Biolley, F., 2004. "Coupling of structure and wake oscillators in vortex-induced vibrations", Journal of Fluids and Structures, Vol.19, pp. 123-140.
- Franzini, G.R., Pereira, A.A.P, Fajarra, A.L.C., and Pesce, C.P., 2008. "Experiments on VIV under frequency modulation". Proceedings of OMAE 07 , 27th Int. Conference on Offshore Mechanics and Arctic Engineering, Estoril, Portugal.
- Fajarra, A.L.C., 2002. "Estudos Experimentais e Analíticos das Vibrações Induzidas pela Emissão de Vórtices em Cilindros Flexíveis e Rígidos", PhD Thesis, Escola Politécnica, University of São Paulo, São Paulo, Brazil.
- Govardhan, R.N. and Williamson, C.H.K., 2006. "Defining the 'modified Griffin plot' in vortex-induced vibration: revealing the effect of Reynolds number using controlled damping", Journal of Fluid Mechanics, Vol. 561, pp. 147-180.
- Huang, N. E., Shen, Z., Long, S.R., Wu, M.C., Shih, H.H., Zheng, Q., Yen, N., Tung, C.C., and Liu, H.H., 1998. "The empirical mode decomposition and the Hilbert spectrum for nonlinear and non-stationary time series analysis", Royal

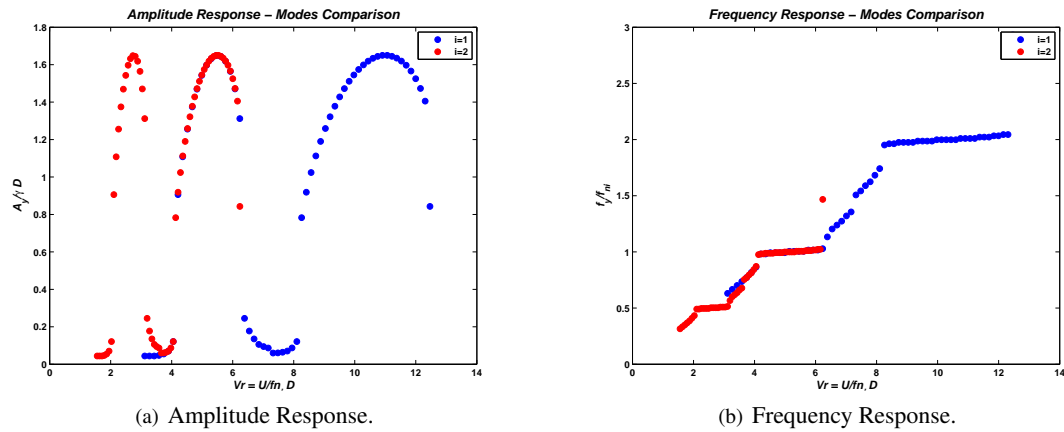


Figure 4. Results for free-oscillations simulations.

Society London, Vol. 454, pp. 403-455.

Iwan, W.D. and Blevins, R.D., 1974, "A Model for Vortex-Induced Oscillation of Structures", Journal of Applied Mechanics, Vol. 41, pp. 581-586.

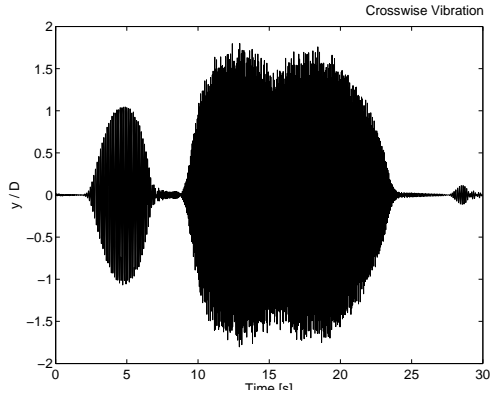
Khalak, A. and Williamson, C.H.K., 1999. "Motions, forces and modes transitions in Vortex-Induced Vibration at low Reynolds Number", Journal of Fluids and Structures, Vol. 13, pp. 813-851.

Parra, P. and Aranha, J.A.P., 1996. "Vibrações Induzidas por Emissão de Vórtices: Modelo Fenomenológico e Experimentos", Technical Report, Departamento de Engenharia Naval e Oceânica, University of São Paulo, São Paulo, Brazil.

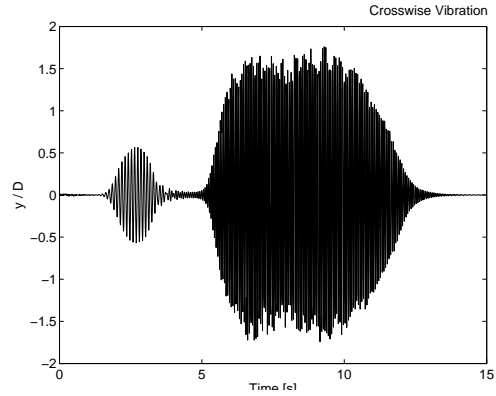
Williamson, C.H.K. and Govardhan, R.N., 2004. "Vortex-Induced Vibrations", Annual Review of Fluids Mechanics, Vol.36, pp. 413-455.

## 7. Responsibility notice

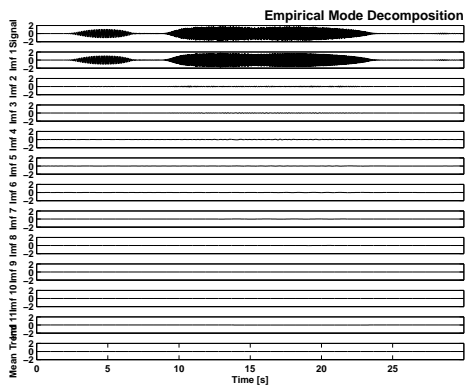
The author(s) is (are) the only responsible for the printed material included in this paper.



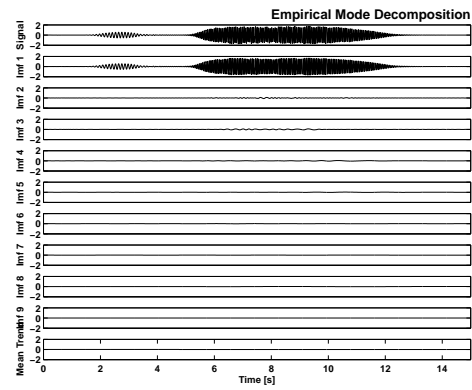
(a) Sim. 1 - Signal.



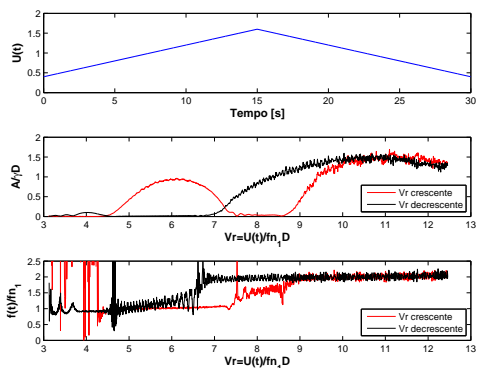
(b) Sim. 2 - Signal.



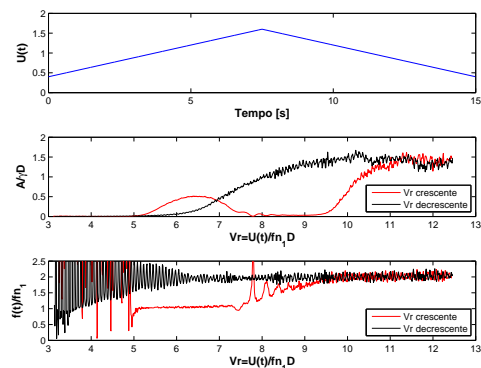
(c) Sim. 1 - IMFs.



(d) Sim. 2 - IMFs.



(e) Sim. 1 - Instantaneous Results.



(f) Sim. 2 - Instantaneous Results.

Figure 5. Results for simulations with time-dependent free stream velocity.